Available online at www.internationaleJournals.com

International eJournals

International eJournal of Mathematics and Engineering 103 (2010) 955 - 966

ISSN 0976 – 1411

INTERNATIONAL eJOURNAL OF MATHEMATICS AND ENGINEERING

www.InternationaleJournals.com

TORQUE RIPPLE REDUCTION BY USING SPACE VECTOR PULSE WIDTH MODULATION FOR VSI FED INDUCTION MOTOR DRIVE

K .Gopala Krishna [(1)]
Assistant Professor-EEE,
Adam's Engineering College,
Paloncha-507115
karanamgopal@yahoo.com
Cell: 9912886388.

P. Venugopal Rao [(2)]
Head of the Department-EEE,
SR Engineering College,
Warangal-506371
pendyalavenu@yahoo.com
Cell: 9440325770.

Abstract: With the Conventional DTC scheme employing a Voltage Source Inverter (VSI), it is possible to control directly the stator flux linkage and the electromagnetic torque by the optimum selection of inverter switching vectors. The selection of inverter switching vector is made to restrict the flux and torque errors within the respective flux and torque hysteresis bands. However, DTC drives utilizing hysteresis comparators suffer from high torque ripple and variable switching frequency. The most common solution to this problem is to use the Space Vector Modulation. This achieves lower switching losses, better DC bus utilization, lower torque ripple, constant switching frequency, lower total harmonic distortion in the motor current. In this paper the modeling & simulation of induction motor drive employing DTC, SVM-DTC was carried out using MATLAB/SIMULINK simulation package and results are compared.
Key words: DTC, VSI, SVM-DTC.

I. INTRODUCTION

Many studies have been developed to find out different solutions for the induction motor control having the features of precise and quick torque response, and reduction of the complexity of field oriented algorithms. The Direct torque control (DTC) technique has been recognized as viable solution to achieve these requirements. The name Direct Torque Control is derived from the fact that, on the basis of error between the reference and the estimated values of torque and flux, it is possible to directly control the inverter states in order to reduce the torque and flux errors with in prescribed limits. In principle the DTC selects one of the six voltage vectors and two zero voltage vectors generated by a VSI in order to keep stator flux and torque within the limits of two hysteresis bands. The right application of this principle allows a decoupled control of flux and torque without the need of coordinate transformation, PWM pulse generation and current regulators. However, the presence of hysteresis controllers leads to a variable switching frequency operation. In addition, the time discretization due to the digital implementation besides the limited number of available voltage vectors determines the presence of current and torque ripple.

In [4,7-9], different methods have been presented which allow constant switching frequency operation. In general, they require control schemes which are more complex with respect to the basic DTC scheme. With reference to current and torque ripple it has been verified that a large influence is exerted by the amplitude of flux and torque hysteresis bands, and the voltage vector selection criteria [3], [11]. It can be noted also that a given voltage vector has a different effect on the drive behavior at high and low speed. Taking these considerations into

account, a good compromise has been obtained using different switching tables at high and low speed [11].

In general, the determination of the switching tables is carried out on the basis of physical considerations concerning the effects determined by radial and tangential variations of the stator flux vector on torque and flux values. Although simple, this approach leads to unexpected torque variations in some particular operating conditions. The understanding of these phenomena requires a rigorous analytical approach taking the electromagnetic behavior of the machine into account [2], [6]. A substantial reduction of current and torque ripple could be obtained using, at each cycle period, a preview technique in the calculation of the stator flux vector variation required to exactly compensate the flux and torque errors [4], [8]. In order to apply this principle, the control system should be able to generate, at each sampling period, any voltage vector (e.g., using the Space Vector Modulation technique).

Several solutions with modified DTC are presented in the literature. DTC can be easily integrated with an artificial intelligence control strategy. The fuzzy logic solution for flux and torque control is shown in [1]. A different approach is to combine the voltage vector selection with an adequate pulse width modulation (PWM) strategy in order to obtain a smooth operation. The closed-loop stator flux predictive control, open-loop torque control using space-vector Modulation (SVM) implementation is shown in [5]. The SVM is a performant open-loop vector modulation strategy [10]. This paper introduces a new direct torque and flux control based on SVM (DTC-SVM) for IM drives. It implements closed-loop control for both flux and torque in a similar manner as DTC, but the voltage is produced by an SVM unit. This way, the DTC transient performance and robustness are preserved and the steady-state torque ripple is reduced. Additionally, the switching frequency is constant and totally controllable.

I. PRINCIPLE OF SVM-DTC

Space Vector Modulation is one of the PWM technique in which, when the drive is excited by 3-ø balanced currents produces a voltage space vector which traces a circle with uniform velocity by sampling that rotating reference voltage space vector with high sampling frequency different switching's can be possible. It is similar to Sine-Triangle PWM in which sinusoidal frequency is proportional to rotating space vector & triangle wave frequency is proportional to sampling frequency.

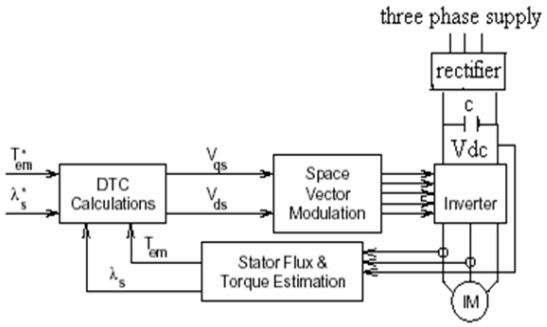

Fig 1. Block Diagram of SVM-DTC

In the block diagram directly AC supply is not connect to Induction Motor because for majority of applications, a wide range of frequency variation is desirable. That's why 3-ø AC is connected diode rectifier which converts AC to DC, diode rectifier because it improves power factor. Rectified DC output is fed to inverter to convert it to AC. They are broadly classified depending upon source feeding them: Voltage or Current source. In both these sources, the magnitude should be adjustable. The output frequency becomes independent of input supply

frequency, by means of dc link. The dc link filter consists of a capacitor to keep the input voltage to the inverter a stiff DC. This is power conversion stage. The torque and flux of induction motor are estimated and they are compared with reference torque and flux, that error is modulated in SVM & fed to the inverter so that respective inverter state is switched.

In case of DC separately excited machine by construction armature and field are orthogonal and it is easily possible to control torque & flux producing components independently. Similar to that for induction machine it is required to resolve stator current into flux producing & torque producing components for independent control.

In detail 3-ø machine dynamic model is complex because the 3-ø rotor winding moves with respect to 3-ø stator winding. So by converting 3-ø machine into equivalent 2-ø machine complexity reduces. Consider a symmetrical three-phase induction machine with stationary as-bs-cs axes at 2π/3-angle apart, as shown in Figure 2. Our goal is to transform the three-phase stationary reference frame (as~bs~cs) variables into two-phase stationary reference frame (d^s~q^s) variables and then transform these to synchronously rotating reference frame (d^e~q^e), and vice-versa.

Assume that the d^s_ q^s Axes are oriented at Θ angle, as shown in Figure .2. The voltages V_{ds}^s and V_{qs}^s can be resolved into as~bs~cs components and can be represented in the matrix form as

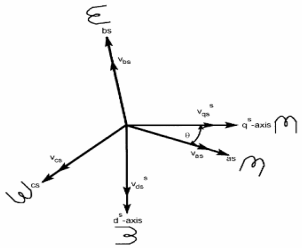

Fig 2. Stationary frame a~b~c to d^s~q^s axes transformation

$$\begin{bmatrix} V_{as} \\ V_{bs} \\ V_{cs} \end{bmatrix} = \begin{bmatrix} \cos\theta & \sin\theta & 1 \\ \cos(\theta-120^0) & \sin(\theta-120^0) & 1 \\ \cos(\theta+120^0) & \sin(\theta+120^0) & 1 \end{bmatrix} \begin{bmatrix} V_{qs}^s \\ V_{ds}^s \\ V_{os}^s \end{bmatrix}$$

The corresponding inverse relation is

$$\begin{bmatrix} V_{qs}^s \\ V_{ds}^s \\ V_{os}^s \end{bmatrix} = (2/3) \begin{bmatrix} \cos\theta & \cos(\theta-120^0) & \cos(\theta+120^0) \\ \sin\theta & \sin(\theta-120^0) & \sin(\theta+120^0) \\ 0.5 & 0.5 & 0.5 \end{bmatrix} \begin{bmatrix} V_{as} \\ V_{bs} \\ V_{cs} \end{bmatrix}$$

Where V_{os}^s is added as the zero sequence component, which may or may not be present.

We have considered voltage as the variable. The current and flux linkages can be transformed by similar equations. It is convenient to set Θ=0, so that the q^s – axis is aligned with the as-axis. Ignoring the zero sequence components, the transformation relations can be simplified as

$$V_{as} = V_{qs}^s, \qquad V_{bs} = -\frac{1}{2}V_{qs}^s - \frac{\sqrt{3}}{2}V_{ds}^s, \qquad V_{cs} = -\frac{1}{2}V_{qs}^s + \frac{\sqrt{3}}{2}V_{ds}^s$$

And inversely

$$V_{qs}^s = \frac{2}{3}V_{as} - \frac{1}{3}V_{bs} - \frac{1}{3}V_{cs} = V_{as} \qquad V_{ds}^s = -\frac{1}{\sqrt{3}}V_{bs} + \frac{1}{\sqrt{3}}V_{cs}$$

In terms of stator resistance & flux linkages

$$V_{qs}^{s} = R_s i_{qs}^{s} + \frac{d}{dt}\psi_{qs}^{s}$$

$$V_{ds}^{s} = R_s i_{ds}^{s} + \frac{d}{dt}\psi_{ds}^{s}$$

$$0 = R_r i_{qr}^{s} + \frac{d}{dt}\psi_{qr}^{s} - \omega_r \psi_{dr}^{s}$$

$$0 = R_r i_{dr}^{s} + \frac{d}{dt}\psi_{dr}^{s} + \omega_r \psi_{qr}^{s}$$

And the torque can be written as $T_e = \frac{3}{2}\left(\frac{P}{2}\right)(\psi_{ds}^{s} i_{qs}^{s} - \psi_{qs}^{s} i_{ds}^{s})$

Firstly model of a three-phase voltage source inverter is presented on the basis of space vector representation is shown in Fig 3. $S_1$to S_6 are the six power switches that shape the output, when top switch is ON taken as 1 & when bottom switch is ON taken as 0. That means for each limb two states are possible, as there are 3 limbs total 2^3 states are possible shown in Fig 4.

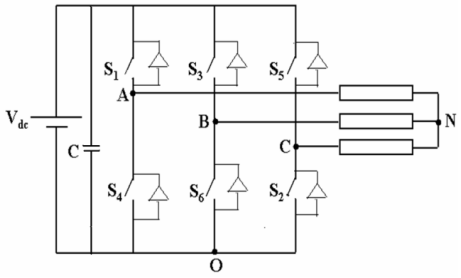

Fig 3. Power circuit of a three-phase VSI

As a result, six non-zero (active) vectors and two zero vectors are possible. Six non-zero vectors (V_1 - V_6) Shape the axes of a hexagonal as depicted in Fig 5. and feed electric power to the system. The angle between any adjacent two non-zero vectors is 60 degrees. Meanwhile,

two zero vectors (V_0 and V_7) are at the origin and apply zero voltage to the load. The eight vectors are called the basic space vectors and are denoted by V_0(000), V_1(100), V_2(110), V_3(010), V_4(011), V_5(001), V_6(101), V_7(111). The same transformation can be applied to the desired output voltage to get the desired reference voltage vector V_{ref} in the d-q plane.

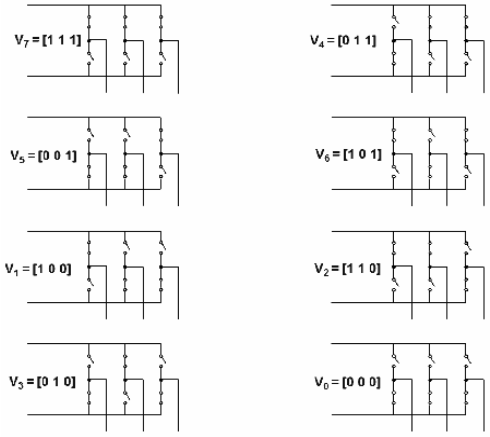

Fig 4. Eight inverter voltages vectors (V_0 to V_7)

The objective of SVPWM technique is to approximate the reference voltage vector V_{ref} using the eight switching patterns. One simple method of approximation is to generate the average output of the inverter in a small period, T to be the same as that of V_{ref} in the same period.

Therefore, space vector PWM can be implemented by the following steps:

Step 1: Determination of V_d. V_q, V_{ref} and angle(α)

Step 2: Determination of time duration T_1, T_2, T_0

Step 3: Determination of the switching time of each switch (S_1 to S_6)

Step 1: Determination of V_d, V_q, V_{ref}, and angle (α)

From Fig 5. we can write

$$V_d = V_{an} - V_{bn} \cdot \cos 60 - V_{cn} \cdot \cos 60$$

$$= V_{an} - \frac{1}{2}V_{bn} - \frac{1}{2}V_{cn}$$

$$V_q = 0 + V_{bn} \cdot \cos 30 - V_{cn} \cdot \cos 30$$

$$= V_{an} + \frac{\sqrt{3}}{2}V_{bn} - \frac{\sqrt{3}}{2}V_{cn}$$

$$\therefore \begin{bmatrix} V_d \\ V_q \end{bmatrix} = \frac{2}{3}\begin{bmatrix} 1 & -\frac{1}{2} & -\frac{1}{2} \\ 0 & \frac{\sqrt{3}}{2} & -\frac{\sqrt{3}}{2} \end{bmatrix}\begin{bmatrix} V_{an} \\ V_{bn} \\ V_{cn} \end{bmatrix}$$

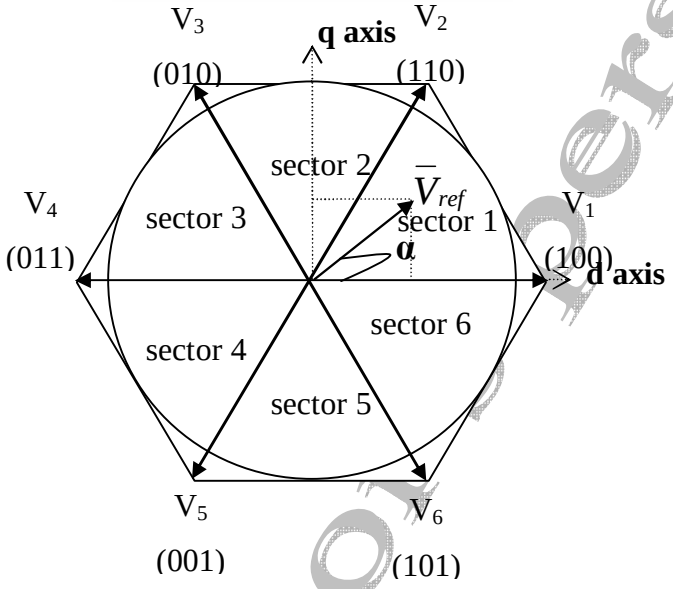

Fig 5. Basic switching vectors and sectors

$$\therefore \alpha = \tan^{-1}\left(\frac{V_q}{V_d}\right) = \omega t = 2\pi f t,$$

where f=fundamental frequency.

Step 2: Determination of time duration T_1, T_2, T_0

From Fig 6. The switching time duration can be calculated as follows:

- Switching time duration at Sector 1

$$\int_0^{T_z} \overline{V}_{ref} = \int_0^{T_1} \overline{V}_1 dt + \int_{T_1}^{T_1+T_2} \overline{V}_2 dt + \int_{T_1+T_2}^{T_z} \overline{V}_0$$

$$\therefore T_z \cdot \overline{V}_{ref} = (T_1.\overline{V}_1 + T_2.\overline{V}_2)$$

$$\Rightarrow T_z \cdot \left|\overline{V}_{ref}\right| \cdot \begin{bmatrix} \cos\alpha \\ \sin\alpha \end{bmatrix} = T_1 \cdot \frac{2}{3} V_{dc} \cdot \begin{bmatrix} 1 \\ 0 \end{bmatrix} + T_2 \cdot \frac{2}{3} \cdot V_{dc} \cdot \begin{bmatrix} \cos(\pi/3) \\ \sin(\pi/3) \end{bmatrix}$$

(where, $0 \le \alpha \le 60°$)

$$\therefore T_1 = T_z \cdot a \cdot \frac{\sin(\pi/3 - \alpha)}{\sin(\pi/3)} \qquad (1a)$$

$$\therefore T_2 = T_z \cdot a \cdot \frac{\sin(\alpha)}{\sin(\pi/3)} \qquad (1b)$$

$$\therefore T_0 = T_z - (T_1 + T_2)$$

$$\left(where \quad T_z = \frac{1}{f_z} \quad and \quad a = \frac{\left|\overline{V}_{ref}\right|}{\frac{2}{3} V_{dc}} \right)$$

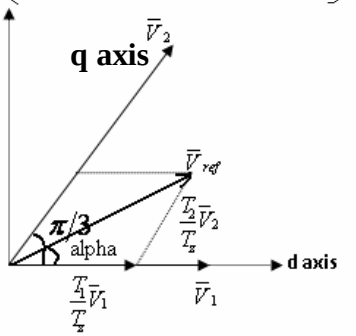

Fig 6. Reference vector as a combination of adjacent vectors at sector-1

Step 3: Determination of the switching time of each switch (S_1 to S_6)

The switching time for each switch is tabulated in Table I. Switching sequence is tabulated in Table II.

Sector	Upper Switches (S_1,S_3,S_5)	Lower Switches (S_4,S_6,S_2)
1	$S_1=T_1+T_2+T_0/2$ $S_3=T_2+T_0/2$ $S_5=T_0/2$	$S_4=T_0/2$ $S_6=T_1+T_0/2$ $S_2=T_1+T_2+T_0/2$
2	$S_1=T_1+T_0/2$ $S_3=T_1+T_2+T_0/2$ $S_5=T_0/2$	$S_4=T_2+T_0/2$ $S_6=T_0/2$ $S_2=T_1+T_2+T_0/2$
3	$S_1=T_0/2$ $S_5=T_2+T_0/2$ $S_3=T_1+T_2+T_0/2$	$S_4=T_1+T_2+T_0/2$ $S_6=T_0/2$ $S_2=T_1+T_0/2$
4	$S_1=T_0/2$ $S_3=T_1+T_0/2$ $S_5=T_1+T_2+T_0/2$	$S_4=T_1+T_2+T_0/2$ $S_2=T_0/2$ $S_6=T_2+T_0/2$
5	$S_3=T_0/2$ $S_1=T_2+T_0/2$ $S_5=T_1+T_2+T_0/2$	$S_6=T_1+T_2+T_0/2$ $S_2=T_0/2$ $S_4=T_1+T_0/2$
6	$S_3=T_0/2$ $S_5=T_1+T_0/2$ $S_1=T_1+T_2+T_0/2$	$S_6=T_1+T_2+T_0/2$ $S_4=T_0/2$ $S_2=T_2+T_0/2$

Table I Switching Time Table at Each Sector

Sector number	ON-sequence	OFF-sequence
1	0-1-2-7	7-2-1-0
2	0-3-2-7	7-2-3-0
3	0-3-4-7	7-4-3-0
4	0-5-4-7	7-4-5-0
5	0-5-6-7	7-6-5-0
6	0-1-6-7	7-6-1-0

Table II Switching Sequence Table

The waveforms considered here are the switching pulses of the upper switches and mirror images represent the pulses of lower switches.

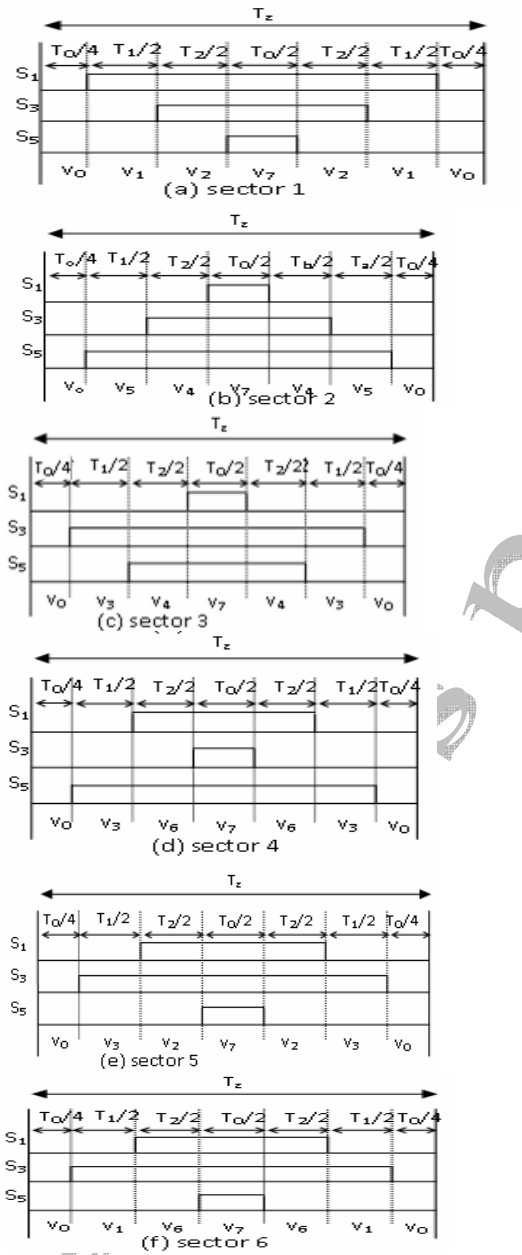

Fig 7. SVPWM switching patterns of upper switches at each sector

II. DC BUS UTILIZATION WITH SVPWM

The principal advantage of the SVPWM over SPWM is that it enhances the DC bus utilization by about 15%. It is instructive to evaluate the sample-averaged pole voltage of a phase, V_{AO} for instance, to understand this fact.

In eqn.1, $|V_{sr}|$ denotes the amplitude of the reference vector and 'α' represents the position of the reference vector with respect to the beginning of the sector in which the tip of the reference vector is situated.

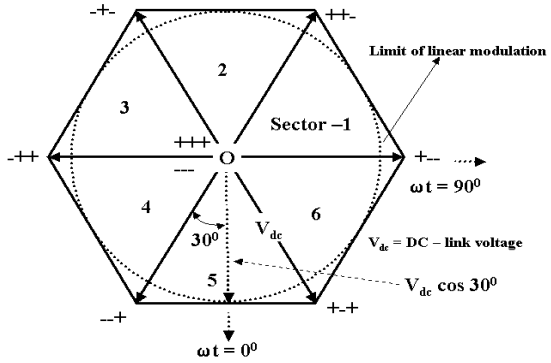

Fig 8. Determination of the sample-averaged pole voltage

During $0^0 \le \omega t \le 30^0$

$$V_{AO,avg} = \frac{V_{dc}/2}{T_s}\left(-\frac{T_0}{2} - T_1 + T_2 + \frac{T_0}{2}\right) \quad (2)$$

$$V_{BO,avg} = \frac{V_{dc}/2}{T_s}\left(-\frac{T_0}{2} - T_1 - T_2 + \frac{T_0}{2}\right) \quad (3)$$

$$V_{CO,avg} = \frac{V_{dc}/2}{T_s}\left(-\frac{T_0}{2} + T_1 + T_2 + \frac{T_0}{2}\right) \quad (4)$$

During $30^0 \le \omega t \le 90^0$

$$V_{AO,avg} = \frac{V_{dc}/2}{T_s}\left(-\frac{T_0}{2} + T_1 + T_2 + \frac{T_0}{2}\right) \quad (5)$$

$$V_{BO,avg} = \frac{V_{dc}/2}{T_s}\left(-\frac{T_0}{2} - T_1 - T_2 + \frac{T_0}{2}\right) \quad (6)$$

$$V_{CO,avg} = \frac{V_{dc}/2}{T_s}\left(-\frac{T_0}{2} + T_1 - T_2 + \frac{T_0}{2}\right) \quad (7)$$

Substituting eqn.1 in eqn. 2 one obtains:

$$V_{AO,avg} = \frac{V_{dc}/2}{T_s} * \frac{|V_{sr}|}{V_{dc}} * \frac{T_s}{\sin 60^0}\left(-\sin(60^0 - \alpha) + \sin\alpha\right) \quad (8)$$

Noting that $\omega t = \alpha - 30^0$, when $\omega t \le 30^0$ and simplifying,

$$V_{AO,avg} = |Vsr| \, Sin\,\omega t \quad (9)$$

Substituting eqn.1 in eqn. 5 one obtains:

$$V_{AO,avg} = \frac{V_{dc}/2}{T_s} * \frac{|V_{sr}|}{V_{dc}} * \frac{T_s}{\sin 60^0}\left(\sin(60^0 - \alpha) + \sin\alpha\right) \quad (10)$$

Noting that $\omega t = \alpha + 30^0$, when $30^0 \le \omega t \le 90^0$ and simplifying,

$$V_{AO,avg} = \frac{|Vsr|}{\sqrt{3}} Sin(\omega t + 30^0) \qquad (11)$$

The average pole voltage variation is plotted in Fig 9. The waveform of the average pole voltage consists of a fundamental component and components of the triplen order.

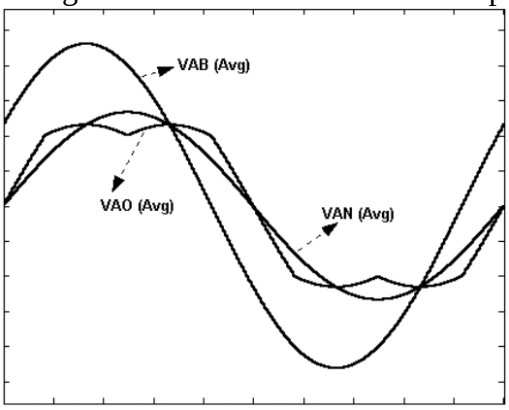

Fig 9. Waveforms of averaged pole voltage, phase voltage and line-line voltage

The waveform of the averaged line-line voltage is sinusoidal as the triplen voltage components of the pole voltages cancel out each other, being cophasal. The averaged phase voltage also remains sinusoidal with a peak value, which is $1/\sqrt{3}$ times that of the peak value of the line-line voltage. The peak value of the A-phase voltage, while the inverter is operated in the range of linear modulation is given by:

$$V_{ph,peak} = (2/3) * |V_{sr}| \qquad (12)$$

Maximum magnitude of the reference voltage space vector corresponds to the radius of the biggest circle that can be inscribed in the hexagon as shown in figure .8. and is equal to, $\sqrt{3}/2V_{dc}$ where V_{dc} is the input DC voltage. Thus, the maximum value of the peak-phase voltage is given by

$$V_{ph,peak,max} = \frac{2}{3} * \frac{\sqrt{3}}{2} * V_{dc} = \frac{V_{dc}}{\sqrt{3}} = 0.577 * V_{dc} \qquad (13)$$

It is known that the maximum value of the peak-phase voltage that can be obtained from a 3-Ph inverter with Sinusoidal Pulse Width Modulation (SPWM) technique is equal to $0.5V_{dc}$ It is therefore evident that SVPWM achieves a better DC bus utilization compared to SPWM (by about 15.4%).

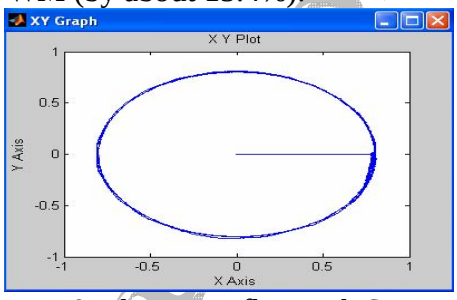

Fig 10. d-q stator flux with SVM-DTC

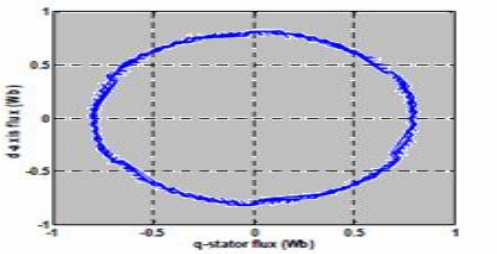

Fig 11. d-q stator flux with a conventional DTC

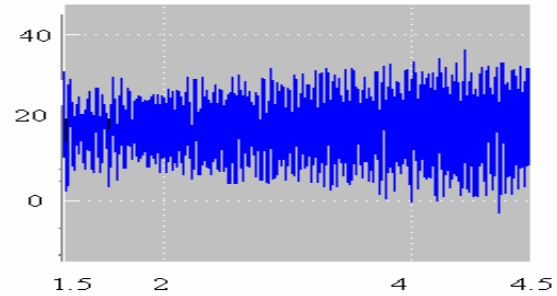

Fig 12. Out put torque with SVM-DTC

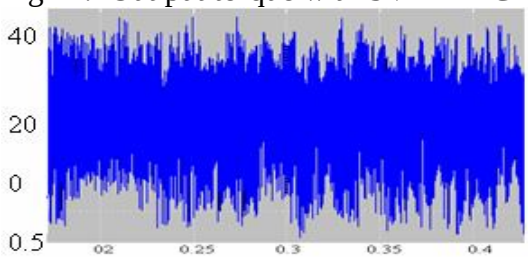

Fig 13. Out put torque with conventional DTC

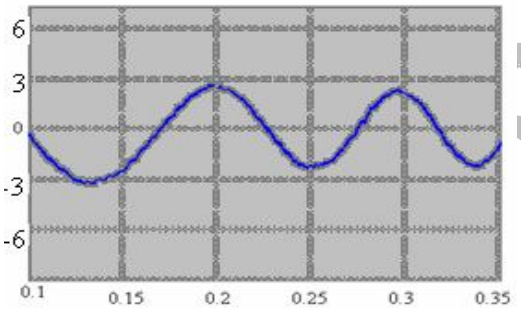

Fig 14. Stator d-current with SVM-DTC

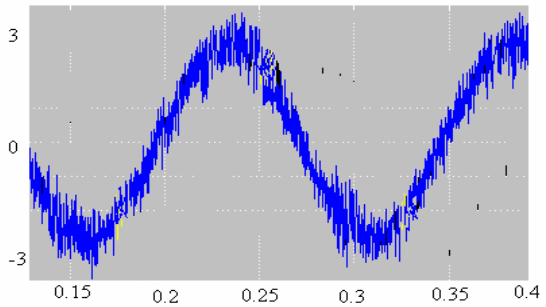

Fig 15. Stator d-current with conventional DTC

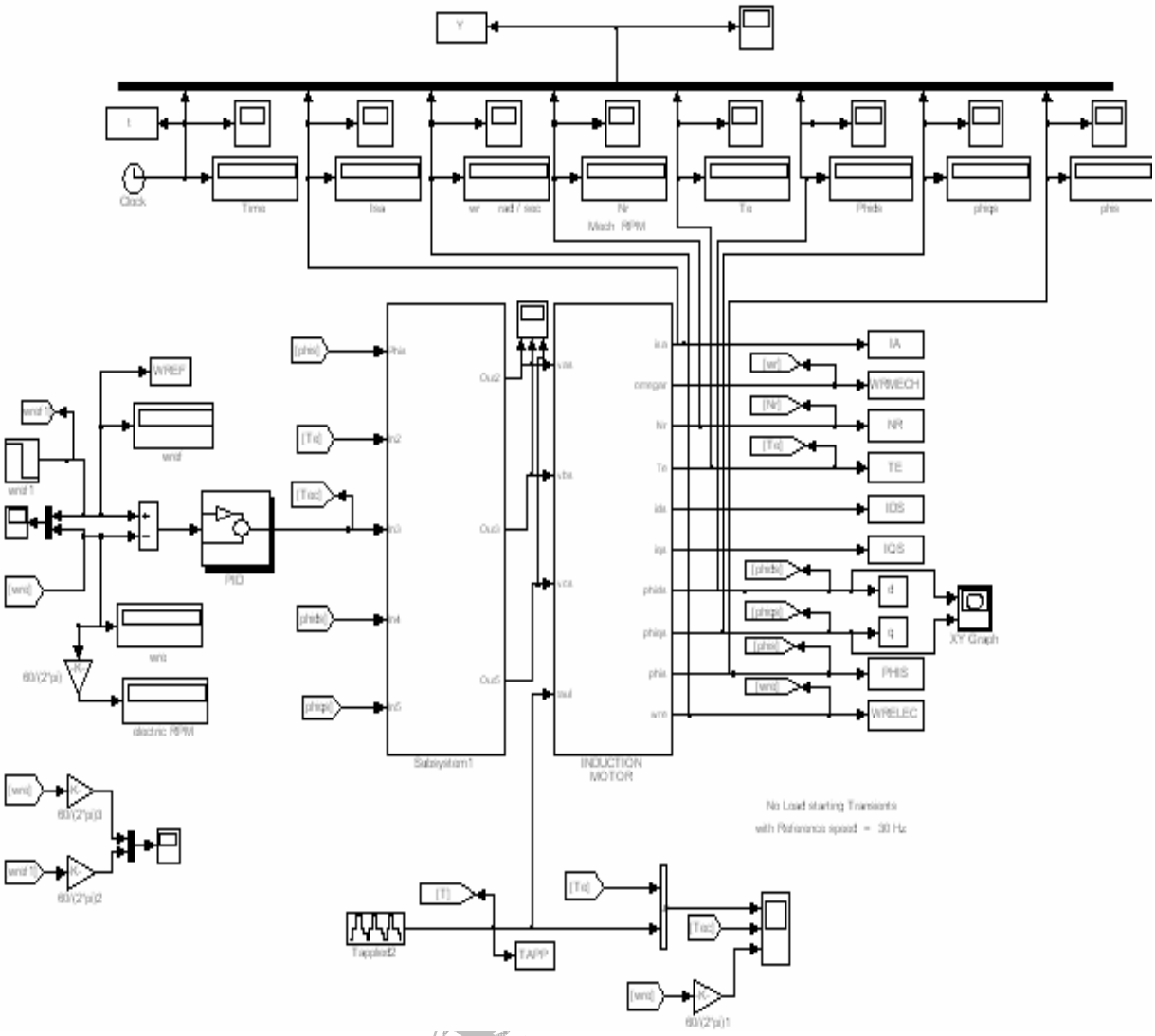

Fig 16. Conventional DTC Simulink model

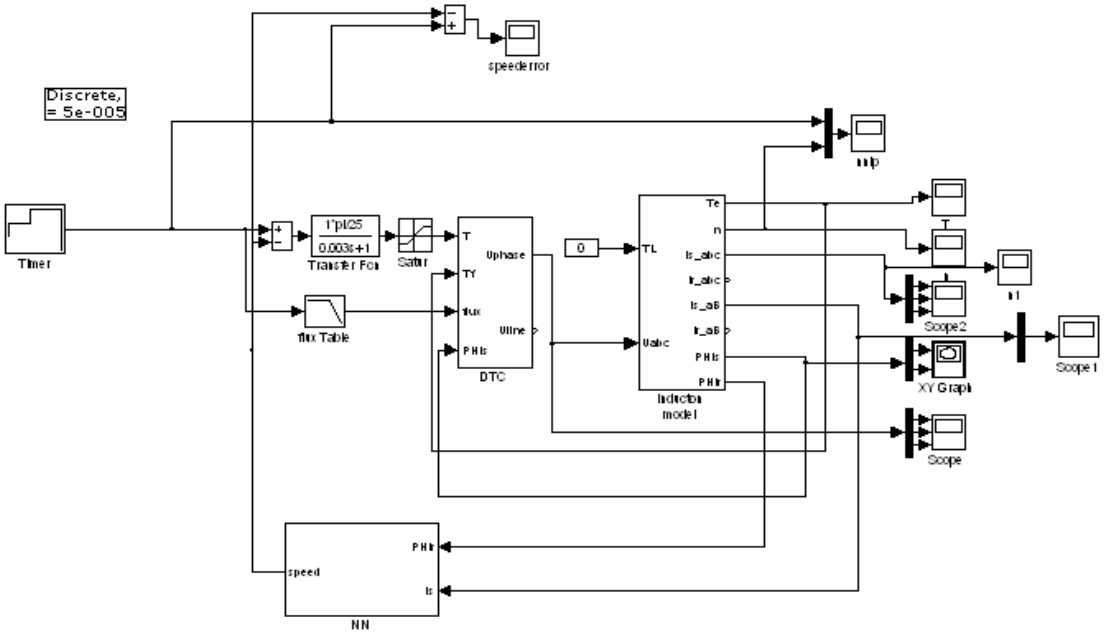

Fig 17. SVM-DTC Simulink model

Simulation was carried out on a 3-ø induction motor having Stator resistance: 2.7Ω, Stator inductance: 0.3562H, Rotor resistance: 2.23 Ω, Rotor inductance: 0.3562H, Mutual inductance: 0.3425H, Frictional coefficient: 0.00825, Number of poles: 2. Switching frequency: 5KHz. Figures 16 & 17 shows Simulink models of conventional DTC, SVM-DTC. Figures 10-15 shows the results of conventional DTC, SVM-DTC.

III. CONCLUSION

In conventional DTC, as the torque ripple is maintained within hysteresis band, switching frequency changes with speed. Moreover, the torque ripple is important problem at low speed. So using constant switching frequency a desired torque ripple can be achieved at low speeds where it really matters. The torque ripple for this SVM-DTC is significantly improved and switching frequency is maintained constant, total harmonic distortion is also reduced. Numerical Simulations have been carried out showing the advantages of the SVM-DTC method with respect to the conventional DTC.

IV. REFERENCES

[1] A. Mir, D. S. Zinger and M. E. Elbuluk "Fuzzy implementation of direct self control of induction motors," *IEEE Trans. Ind. Applicat.*, vol. 30, May/June'94.

[2] A. Tani, D. Casadei, and G. Serra "Analytical investigation of Torque and flux ripple in DTC schemes for induction motors," in *Proc. IECON'97*, New Orleans, LA.

[3] A. Tani, D. Casadei, G. Grandi, and G. Serra "Effects of flux And torque hysteresis band amplitude in direct torque control Of induction machines," in *Proc. IECON'94*, Bologna, Italy, Sept. 5–9, 1994.

[4] A. Tani, D. Casadei and G. Serra "Stator flux vector control for high performance induction motor drives using space vector modulation," *Electromotion*, vol. 2, no. 2.

[5] A. Tani, D. Casadei, and G. Sera "Stator flux vector control For high performance induction motor drives using space vector modulation," in *Proc. OPTIM'96*.

[6] B. de Fornel, E. V. Westerholt, I. El Hassan and X. Roboam "Torque dynamic behavior of induction machine DTC in 4 Quadrant operation," in *Proc. ISIE'97*, Guimaraes, Portugal, July 7-11'97.

[7] C. Lochot, P. Maussion and X. Roboam "A new direct torque control strategy for an induction motor with constant switching frequency operation," in *Proc. EPE'95*, Sevilla, Spain.

[8] "Constant frequency operation of a DTC induction motor drive for electric vehicle," in *Proc. ICEM'96*, vol. III, Vigo, Spain, Sept.10–12'96.

[9] F. Profumo, L. M. Tolbert, M. Pastorelli, and T. G. Habetler "Direct torque control of induction machines using space vector modulation," *IEEE Trans. Ind. Applicat.*, vol. 28, Sept./Oct.'92.

[10] J. K. Pedersen and P. Thoegersen " Stator flux oriented asynchronous vector modulation for AC-drives," in *Proc. IEEE PESC'90*.

[11] "Switching strategies in direct torque control of induction machines," in *Proc. ICEM'94*, Paris, France, Sept. 5–8'94.

[12] K. Gopala Krishna, Prof. P. Venugopal Rao "Space Vector Pulse Width Modulation for Two Level Inverter feeding Induction Motor" in proceedings of National Conference on Emerging Technologies in Electrical Engineering, June11^{th} –12^{th} , 2010.